nature
structural &
molecular biology

Dynamically driven protein allostery

Nataliya Popovych[1], Shangjin Sun[1], Richard H Ebright[2] & Charalampos G Kalodimos[1]

Allosteric interactions are typically considered to proceed through a series of discrete changes in bonding interactions that alter the protein conformation. Here we show that allostery can be mediated exclusively by transmitted changes in protein motions. We have characterized the negatively cooperative binding of cAMP to the dimeric catabolite activator protein (CAP) at discrete conformational states. Binding of the first cAMP to one subunit of a CAP dimer has no effect on the conformation of the other subunit. The dynamics of the system, however, are modulated in a distinct way by the sequential ligand binding process, with the first cAMP partially enhancing and the second cAMP completely quenching protein motions. As a result, the second cAMP binding incurs a pronounced conformational entropic penalty that is entirely responsible for the observed cooperativity. The results provide strong support for the existence of purely dynamics-driven allostery.

Allosteric regulation is widely used in biological systems as an effective mechanism to control protein activity[1–4]. Although numerous allosteric systems have been studied for many decades, the mechanisms that underlie the communication between distant sites and energetically couple them remain largely elusive. According to the classical 'mechanical' view, allosteric interactions are mediated by a series of discrete conformational changes that alter protein structure[5–7]. Because allostery is fundamentally thermodynamic in nature, long-range communication may be mediated not only by changes in the mean conformation (enthalpic contribution) but also by changes in the dynamic fluctuations about the mean conformation (entropic contribution)[8,9]. The current view of allostery tends to explain the phenomenon only in pure structural terms, neglecting the important role of protein motions. At the other extreme, allosteric processes could, in theory, proceed solely through changes in protein dynamics in the absence of conformational changes[10]. Although there is increasing evidence suggesting a role of conformational dynamics in cooperative ligand-binding processes[8,11–17], hitherto it has not been known whether dynamic phenomena can dominate allosteric mechanisms in proteins. Here, we present direct experimental evidence that allostery can be mediated solely by changes in protein dynamics.

Typically, studies of systems showing homotropic cooperativity have focused on comparison of unliganded beginning and ligand-bound end states. However, the key conformational state with the potential to provide detailed insight into the mechanisms underpinning the allosteric process is the intermediate state. These states cannot be isolated in positively cooperative proteins because the singly liganded intermediates are poorly populated. In contrast, negatively cooperative systems allow, in principle, for the isolation and characterization of intermediates states[14,18]. We have exploited the strong negative cooperativity of cAMP binding to CAP to 'freeze' binding conformations at intermediate stages and used NMR and isothermal titration calorimetry (ITC) to assess the role of structure and dynamics in allosteric cooperativity. CAP is a transcriptional activator that exists as a homodimer in solution (K_d of the dimer is $\sim$0.03 nM)[19], with each subunit comprising a ligand-binding domain at the N terminus (CAP^N; **Supplementary Fig. 1** online), which is also responsible for the dimerization of the protein, and a DNA-binding domain at the C terminus[20,21]. Two cAMP molecules bind dimeric CAP with negative cooperativity and function as allosteric effectors by increasing the protein's affinity for DNA[20]. The distance between the phosphate groups of the two bound cAMP molecules is more than 24 Å (ref. 21); therefore, coulombic interactions cannot contribute to the negative cooperativity. cAMP likewise shows strong negative cooperativity in its interaction with the isolated dimeric CAP^N (ref. 22).

To directly characterize the changes in protein structure and dynamics as a function of the ligation state, we analyzed each of the three distinct conformational states of the dimeric CAP^N (residues 1–138) along the cooperative reaction coordinate: that is, the unliganded state (apo-CAP^N), the singly liganded (intermediate) state ($cAMP_1$–CAP^N) and the doubly liganded state ($cAMP_2$–CAP^N). The isolation and characterization of these states allowed us to probe directly the effect induced by the binding of the first ligand molecule on the second, unliganded site. We found that binding of the first cAMP molecule has no or minimal effects on the conformation of the second binding site. Instead, a distinct change in protein motions between the two sequential cAMP binding steps results in a large difference in conformational entropy. Thermodynamic analysis confirms that the observed negative cooperativity is driven entirely by changes in entropy.

[1]Department of Chemistry, Rutgers University, Newark, New Jersey 07102, USA. [2]Howard Hughes Medical Institute, Waksman Institute, and Department of Chemistry, Rutgers University, Piscataway, New Jersey 08854, USA. Correspondence should be addressed to C.G.K. (babis@andromeda.rutgers.edu).

Received 9 June; accepted 17 July; published online 13 August 2006; doi:10.1038/nsmb1132

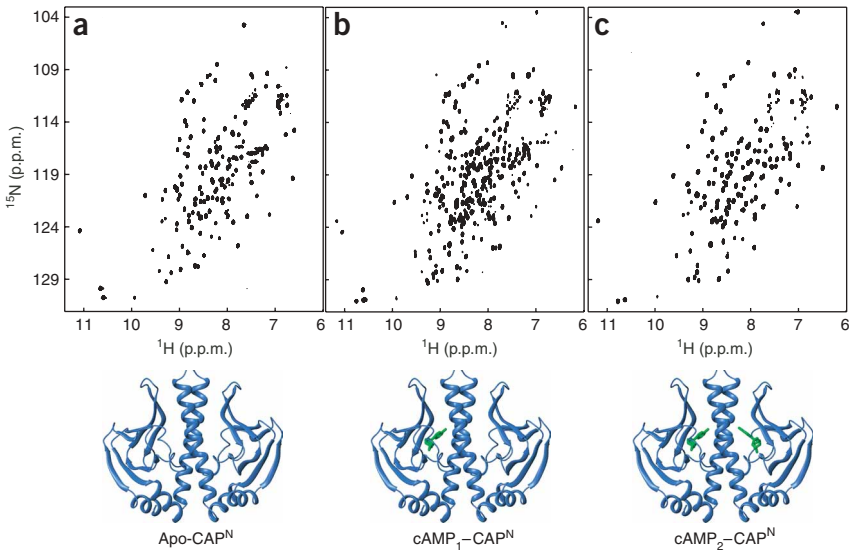

Figure 1 Distinct conformational states of CAP^{N}. (**a**–**c**) 2D ^{1}H-^{15}N HSQC spectra of U-^{2}H,^{15}N-labeled apo-CAP^{N} (**a**), cAMP$_1$–CAP^{N} (**b**) and cAMP$_2$–CAP^{N} (**c**). Molecular models were drawn using the structure of cAMP$_2$–CAP (PDB entry 1G6N). cAMP is shown as green sticks.

RESULTS

cAMP binding to CAP^{N} yields distinct conformational states

We have recorded 2D ^{1}H-^{15}N HSQC spectra of CAP^{N} in three states: apo-CAP^{N}, cAMP$_1$–CAP^{N} and cAMP$_2$–CAP^{N} (**Fig. 1**). Only one set of resonances is present for both subunits of CAP^{N} in the unliganded state, suggesting that apo-CAP^{N} exists as a symmetric dimer with identical ligand-binding sites (**Fig. 1a**). Binding of the first cAMP molecule to CAP^{N} gives rise to the intermediate-state complex, cAMP$_1$–CAP^{N}; because of the strong negative cooperativity, only one of the two subunits is occupied. As expected for an asymmetric dimer, the chemical shift degeneracy is lifted and two sets of resonances are observed for the two subunits of the dimer: one set identical to that observed with apo-CAP (assigned to the the unliganded subunit) and one set markedly different from that observed with apo-CAP^{N} (assigned to the liganded subunit) (**Fig. 1b** and **Supplementary Fig. 2** online). Binding of the second cAMP molecule to yield the cAMP$_2$–CAP^{N} complex restores the symmetry of the protein dimer to a conformation identical to that of the liganded subunit in the cAMP$_1$–CAP^{N} complex (**Fig. 1c**). Both cAMP-binding reactions are very slow on the NMR timescale.

Further analysis of the chemical shift behavior of CAP^{N} during its sequential interaction with cAMP (**Supplementary Fig. 2**) provides unambiguous evidence of the strong negative cooperativity, in agreement with previous biochemical data[22]. The key to discriminating between negative and positive cooperativity is to study the complex at a 1:1 stoichiometric ratio of cAMP to CAP^{N} (dimer). If cAMP bound CAP^{N} with positive cooperativity, two species would be present at this ratio: apo-CAP^{N} and cAMP$_2$–CAP^{N}. As both cAMP binding steps are slow on the NMR timescale, 50% of the CAP^{N} would remain in the apo state; that is, the resonances would not be affected by the presence of cAMP. However, this is not what we observed. The unfilled subunit at the 1:1 cAMP/CAP^{N} ratio is clearly affected, as many residues at the interface with the liganded subunit substantially change their chemical shift (**Supplementary Fig. 2**). These results demonstrate that there is only one protein complex present in solution at the 1:1 cAMP/CAP^{N} ratio, corresponding to the intermediate cAMP$_1$–CAP^{N} complex. Therefore, cAMP binds CAP with strong negative cooperativity.

Effect of sequential cAMP binding on the structure of CAP^{N}

To assess the effect on protein structure of the sequential binding of the first and second cAMP molecules to CAP^{N}, we have used chemical shift mapping. The exquisite sensitivity of chemical shift to the environment ensures that considerable shifts would take place if changes in the mean protein conformation occurred upon ligand binding. The effect of the first cAMP binding to the liganded subunit is pronounced throughout the whole monomer, as evidenced by the observed widespread chemical shift changes (**Fig. 2**). In contrast, the unliganded subunit in the cAMP$_1$–CAP^{N} complex is slightly perturbed only at its long C helix, which forms the dimer interface. None of the residues in the β-roll or the phosphate-binding cassette motif, the most conserved and important region in the protein for its interaction with cAMP, is affected. Further examination of the chemical shift behavior of CAP^{N} during its sequential interaction with cAMP demonstrates that the effect of cAMP binding on protein structure is confined, in each step, to only the interacting subunit (**Supplementary Fig. 2**). Thus, the mean conformation of the unfilled cAMP site at the unliganded subunit of the cAMP$_1$–CAP^{N} complex is not at all affected by the presence of the first cAMP, suggesting that the contribution of the 'structural' component to the observed negative cooperativity is negligible.

Effect of sequential cAMP binding on slow protein motions

To understand how protein dynamics adjust along the cooperative reaction coordinate, we characterized the backbone motions of CAP^{N}

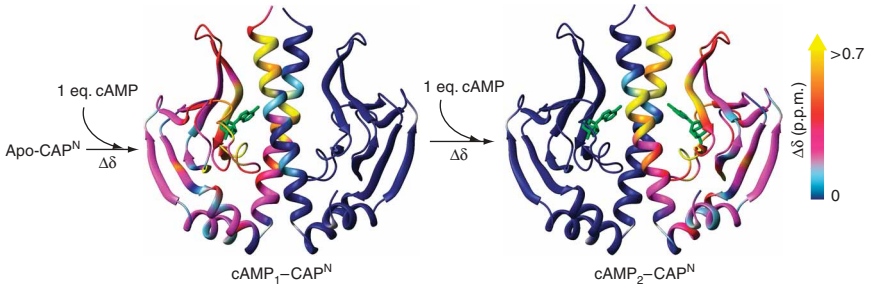

Figure 2 Effect of sequential cAMP binding on the structure of CAP^{N}, assessed by chemical shift mapping. Structures are colored by Δδ (p.p.m.), as follows: dark blue, $\Delta\delta \sim 0$; light blue, $0.02 < \Delta\delta < 0.08$; magenta, $0.08 < \Delta\delta < 0.2$; red, $0.2 < \Delta\delta < 0.4$; orange, $0.4 < \Delta\delta < 0.6$; yellow, $\Delta\delta > 0.7$. Δδ for the cAMP$_2$–CAP^{N} complex reflects the binding effect of the second cAMP molecule on the cAMP$_1$–CAP^{N} complex. Proline residues are colored white.

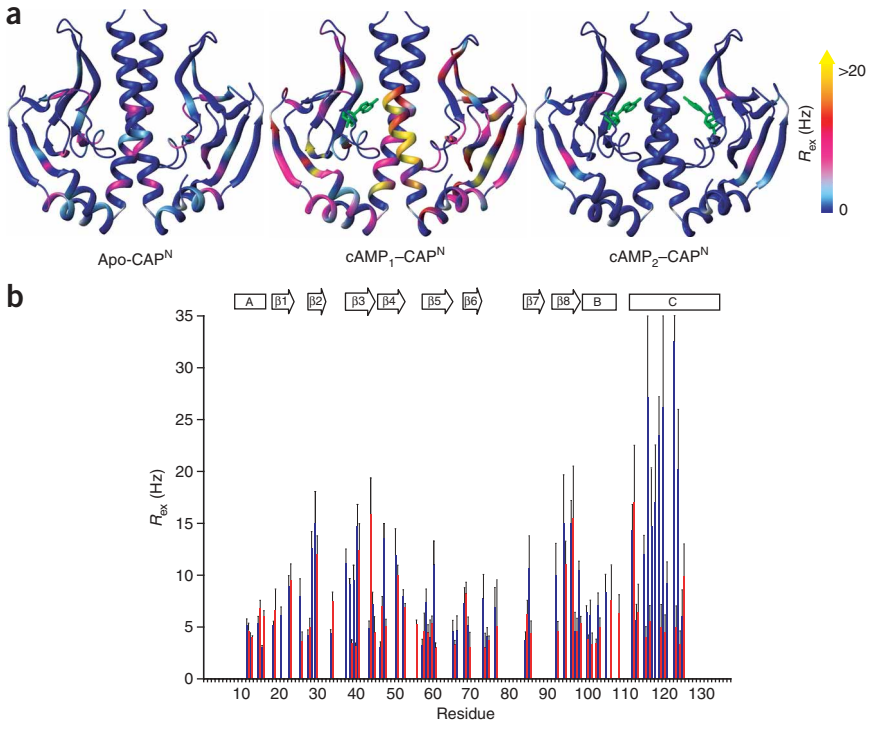

Figure 3 Effect of sequential cAMP binding on the slow motions of CAP^N. (**a**) Conformational exchange dynamics on the µs–ms timescale, as indicated by R_{ex}, are mapped on structures of the protein in the three ligation states. Low values indicate rigidity, whereas higher values indicate flexibility. Color coding by R_{ex} (in Hz) is as follows: dark blue, $R_{ex} \sim 0$; light blue, $1 < R_{ex} < 4$; magenta, $4 < R_{ex} < 8$; red, $8 < R_{ex} < 12$; orange, $12 < R_{ex} < 16$; yellow, $R_{ex} > 16$. (**b**) R_{ex} for the singly liganded $cAMP_1$-CAP^N complex, plotted against residue number. Red and blue represent liganded and unliganded subunits, respectively. Only residues with $R_{ex} > 2$ Hz are shown. Secondary structure boundaries (top) are from the X-ray structure of $cAMP_2$–CAP complex (PDB entry 1G6N).

as a function of the cAMP ligation state, over a wide range of functionally relevant timescales, by measuring relaxation rates (**Supplementary Fig. 3** online). Slow domain motions on the micro- to millisecond (µs–ms) scale are biologically very important because they are close to the timescales on which functional processes take place, such as docking, protein folding and allosteric transitions[23–26]. Upon binding of the first cAMP to CAP^N, resonances for backbone residues of both subunits undergo extensive peak broadening (**Supplementary Fig. 4** online). This indicates substantial conformational exchange, identified by the high magnitude of the term R_{ex} (**Fig. 3**). The contribution to R_{ex} from cAMP binding and dissociation is negligible (see **Supplementary Discussion** and **Supplementary Fig. 5** online). Thus, the pronounced increase of R_{ex} for almost all residues of both subunits means that the protein in the $cAMP_1$–CAP^N complex populates an ensemble of alternate conformations that interconvert on the µs–ms timescale. These slow motions are activated by the first cAMP binding.

Notably, despite the fact that binding of the first cAMP molecule cannot induce long-range structural effects in the other subunit (**Fig. 2**), the dynamics of the system respond to the binding in a highly cooperative way, emphasizing their allosteric character. Residues of the unliganded subunit in the $cAMP_1$–CAP^N complex that are located as far as 35 Å from the bound cAMP (for example, Tyr23, Leu29 and Ile30) show enhanced dynamics. Moreover, the prominent conformational dynamics on the µs–ms timescale exhibited by almost all residues in $cAMP_1$–CAP^N are completely quenched upon binding of the second cAMP molecule to yield the $cAMP_2$–CAP^N complex (**Fig. 3**).

Both subunits undergo the same conformational exchange

To better understand the conformational process that results in such a dramatic change in slow motions of the singly liganded $cAMP_1$–CAP^N complex, we performed a series of relaxation dispersion experiments (**Fig. 4**)[27]. The additional line broadening of NMR signals (R_{ex}) caused by conformational exchange between the ground and an excited state depends on the sum of forward and reverse rates of interconversion (k_{ex}), the relative populations of the exchanging species (p_A and p_B) and the chemical shifts between the exchanging species ($\Delta\omega$) (ref. 27). Because the conformational exchange process is in the fast-exchange limit, only k_{ex} and the product $p_A p_B(\Delta\omega)^2$ can be measured. k_{ex} seems to be similar for most of the residues in the liganded subunit, as the majority of the residues with appreciable R_{ex} can be fitted with k_{ex} values ranging from 900 to 1,600 s^{-1} (**Fig. 4a**). Therefore, it seems that most of the residues in the liganded subunit report on the same exchange process. Assuming a population of 10% ($p_B \sim 0.1$) for the excited state, an estimation of $\Delta\omega$ can then be made. The ^{15}N chemical shift difference ($\Delta\omega$) between the two exchanging conformations may be as high as 4 p.p.m. for residues with large R_{ex} values ($\sim$10–15 Hz), implying major structural rearrangements. If the population of the excited state (p_B) is less than 10%, then even larger $\Delta\omega$ values would be present. As in the case of the liganded subunit, k_{ex} for most residues in the unliganded subunit can be fitted using k_{ex} values ranging from 1,000 to 1,500 s^{-1}. Another, smaller group of residues in the unliganded subunit (for example, Ile106; **Fig. 4b**) seem to have k_{ex} values close to 2,000 s^{-1}. It is possible that these few residues are affected by another, faster process. However, considering the uncertainty, almost all residues can be considered to exchange between the sites with similar k_{ex}. Therefore, it is very likely

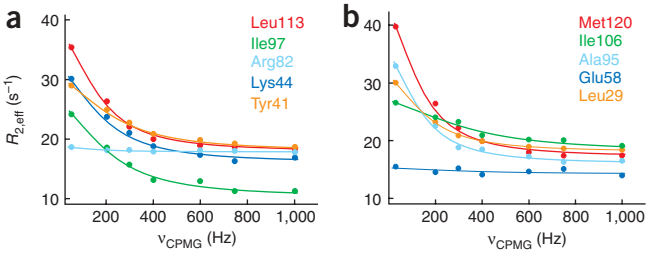

Figure 4 CPMG relaxation dispersion data of ^{15}N backbone amides of CAP^N. (**a**,**b**) Representative curves for residues of the liganded (**a**) and unliganded (**b**) subunits of the $cAMP_1$–CAP^N complex. k_{ex} (s^{-1}) is as follows: Leu113, 1,100 ± 320; Ile97, 1,350 ± 290; Lys44, 1,200 ± 250; Tyr41, 1,150 ± 240; Met120, 1,100 ± 330; Ile106, 1,820 ± 360; Ala95, 1,180 ± 220; Leu29, 1,3200 ± 240.

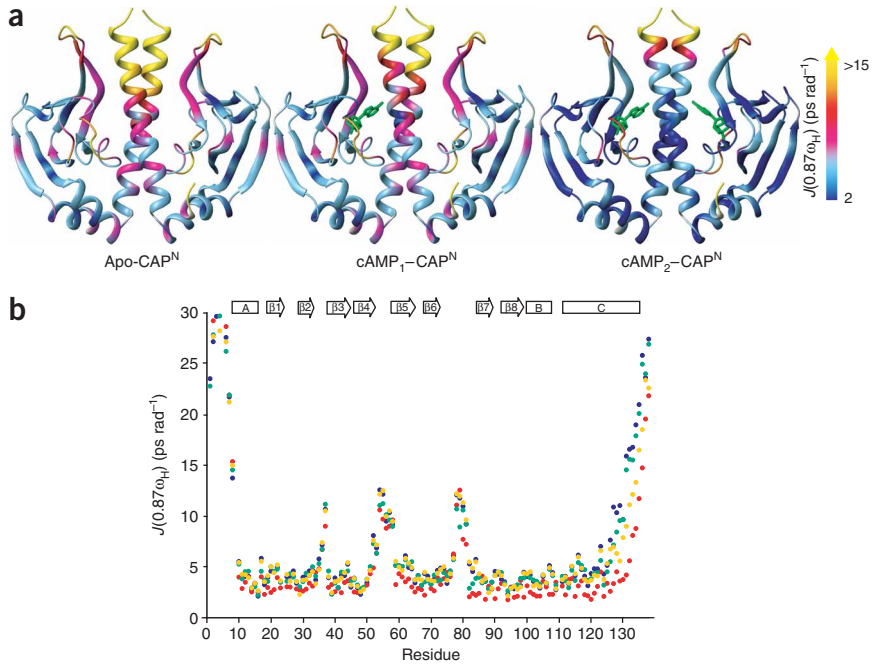

Figure 5 Effect of sequential cAMP binding on the fast motions of CAP^N. (**a**) $J(0.87\omega_H)$, the spectral density function indicating amplitude of motions on the ps–ns timescale, is mapped by continuous-scale color onto structures in the three ligation states. Low values indicate rigidity, whereas higher values indicate flexibility. (**b**) $J(0.87\omega_H)$ plotted against residue number. Blue, apo-CAP^N; green, liganded subunit of cAMP$_1$–CAP^N; orange, unliganded subunit of cAMP$_1$–CAP^N; red, doubly liganded cAMP$_2$–CAP^N. Secondary structure elements are shown as in **Figure 3**.

that all residues of the cAMP$_1$–CAP^N complex, both from the liganded and the unliganded subunits, report on the same conformational exchange process. This is corroborated by the observation that residues located at the dimer interface have very similar k_{ex} values.

Effect of sequential cAMP binding on fast protein motions

Next, we measured changes in motions on the pico- to nanosecond (ps–ns) timescale of the backbone of CAP^N as a function of the ligation state (**Fig. 5**). Motions on this fast timescale are biologically very important because of their strong effect on the entropy of the system[28,29]. Even small changes of these motions have been shown to result in significant entropic changes capable of driving binding processes[30–32]. The conformational flexibility of CAP^N on the ps–ns timescale, as indicated by the spectral density function $J(0.87\omega_H)$, is illustrated in **Figure 5**. Our data show that binding of the first cAMP molecule to yield the cAMP$_1$–CAP^N complex does not affect these motions appreciably (**Fig. 5**). The effect is local and is confined within the cAMP-binding site, where only few residues rigidify their backbones. Residues 80–84 at the phosphate-binding cassette motif of the liganded subunit and 126–133 at the C terminus of the unliganded subunit are the only ones that slightly dampen their fast motions in the singly liganded complex. In contrast to the slow motions (**Fig. 3**), the ps–ns dynamics of the core of the unliganded subunit are not perturbed. Notably, binding of the second cAMP molecule causes widespread stiffening of the backbone in both subunits (**Fig. 5**). The extensive suppression of protein motions throughout the whole molecule attests, once again, to the allosteric nature of protein motions and their exceptional capacity to serve as a carrier of allosteric energy.

Effect of cAMP binding on the native-state ensemble

To directly probe the native-state conformational ensemble of CAP^N, we measured NMR-detected hydrogen-deuterium (H/D) exchange rates of the backbone amides of CAP^N as a function of the cAMP ligation state. The native-state ensemble of a protein consists of an equilibrium of conformational states, and its redistribution upon ligand binding has been suggested to impinge on cooperativity[11,12,33–35]. Fluctuations of the structures allow the amide sites to sample many conformations, some of which permit exchange with the solvent. Therefore, amide exchange rates can reflect dynamic motions over a wide range of timescales that are not accessible by relaxation methods. Binding of the first cAMP molecule to CAP^N results in a slight decrease in exchange rates of the residues in the liganded subunit (**Fig. 6**). However, the unliganded subunit remains largely unaffected. Notably, binding of the second cAMP molecule results in substantial and global decreases in exchange rates of residues in both subunits. Residues at the dimer interface show the most pronounced increase in protection from solvent, indicating optimization of the packing interactions at the interface only when both subunits are filled

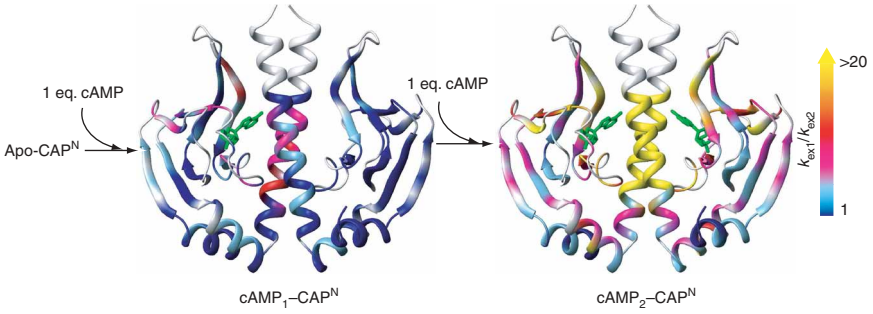

Figure 6 Effect of sequential binding of cAMP to CAP^N on amide exchange rates, shown as the k_{ex1}/k_{ex2} ratio for binding of each cAMP molecule (where k_{ex1} and k_{ex2} are exchange rates before and after cAMP binding, respectively). Lower exchange rates indicate higher protection of amide hydrogens against exchange with solvent deuterons. Thus, higher values of k_{ex1}/k_{ex2} indicate decreased protein flexibility and increased protection induced by cAMP binding. Greater protection arises from narrowing of the population of protein conformational ensembles, so that conformations in which exchange take place are less populated. k_{ex1}/k_{ex2} is mapped onto structures by continuous-scale color; residues with no detectable protection are colored white. Because exchange rates were measured for all states (apo-CAP^N, cAMP$_1$–CAP^N and cAMP$_2$–CAP^N) under identical conditions, k_{ex} values can be directly compared.

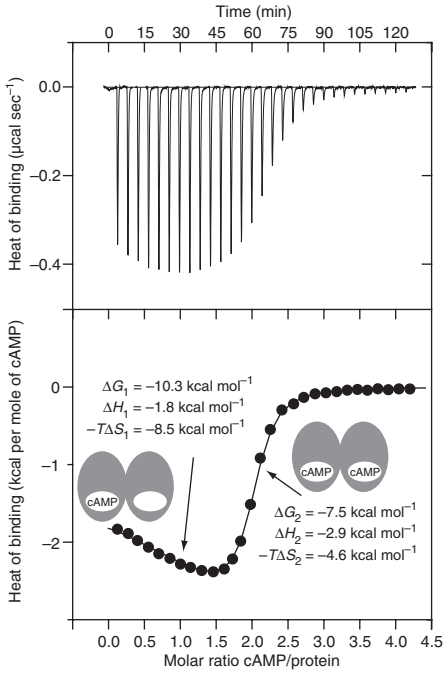

Figure 7 Energetics of cooperative sequential binding of cAMP to CAP^N. ITC traces (top) and binding isotherm (bottom) of the calorimetric titration of cAMP into CAP^N. Solid line in bottom chart represents the fit to a sequential binding site model. K_d = 0.04 μM and 4 μM for the first and second cAMP binding steps, respectively.

with cAMP. We conclude that a considerable reduction in the number of conformational states occurs in the cAMP$_2$–CAP^N complex, but not in the intermediate cAMP$_1$–CAP^N complex. Once again noteworthy are the distinct effects of sequential cAMP binding events on the stability of the protein, with only the second cAMP being capable of eliciting long-range effects.

Thermodynamic basis of the negatively cooperative binding

To determine the thermodynamic basis for the observed anticooperative binding of cAMP to CAP^N, we used high-sensitivity ITC to measure the association free energy, ΔG, and its enthalpic and entropic components, ΔH and ΔS. The biphasic nature of the isotherm (**Fig. 7**) clearly points to the existence of two nonequivalent sites in CAP^N with a large difference in affinity for cAMP. The difference in the free energy change between the two binding steps, $\Delta G_1 - \Delta G_2$, is –2.8 kcal mol^{-1}, resulting in the second cAMP molecule binding CAP^N with a 100-fold lower affinity than the first cAMP. Binding of the second cAMP is accompanied by a more favorable enthalpy change, which, in line with the chemical shift mapping results, argues against its site being distorted as a result of the first cAMP binding. In fact, the measured enthalpy change between the two binding steps ($\Delta H_1 - \Delta H_2 = +1.1$ kcal mol^{-1}) opposes the observed allosteric phenomenology and favors positive rather than negative cooperativity. By contrast, the second cAMP binds CAP^N with a much less favorable entropy change than the first cAMP, amounting to an entropic penalty of $\Delta(-T\Delta S) = 4$ kcal mol^{-1} (where T is temperature). Thus, the thermodynamic basis for the observed negative cooperativity is entirely entropic in nature.

Conformational entropy change upon cAMP binding

The present findings suggest that the observed extensive changes in protein motions are the most probable source of the large difference in entropy change between the two cAMP binding steps. To assess the contribution of protein motions to the conformational entropy of the system[36,37], we calculated changes in order parameters for the first and second cAMP binding to CAP^N (**Fig. 8** and **Supplementary Fig. 6** online). The order parameter, S^2, is a measure of the amplitude of internal motions on the ps–ns timescale and may vary from $S^2 = 1$, for a bond vector having no internal motion, to $S^2 = 0$, for a bond vector rapidly sampling multiple orientations[28]. Binding of the first cAMP to CAP^N results in small increases in S^2, confined primarily to the binding site (**Fig. 8**). In contrast, binding of the second cAMP molecule causes a widespread increase in S^2 (**Fig. 8**), indicating a global rigidification of the protein, in agreement with the $J(0.87\omega_H)$ data (**Fig. 5**). By converting order parameters to entropy (see Methods), we estimate that binding of the first cAMP molecule to CAP^N is accompanied by a conformational entropic penalty $-T\Delta S_{conf1} = 3.2$ kcal mol^{-1}, whereas binding of the second cAMP molecule incurs a much higher entropic penalty, $-T\Delta S_{conf2} = 18.1$ kcal mol^{-1} (**Fig. 8**). Note that conformational entropy estimated through order parameters should be taken as an upper-bound estimate, because the approach assumes that motions are uncorrelated[28,32]. Thus, the extensive difference in S^2 is translated to a very large decrease in the conformational entropy of the system, amounting to $-T\Delta S_{conf} \sim 15$ kcal mol^{-1}, in going from the cAMP$_1$–CAP^N to the cAMP$_2$–CAP^N state. We conclude that the calorimetrically measured entropic penalty that accompanies anticooperative cAMP binding is indeed dominated by the unfavorable conformational entropy change upon binding of the second cAMP to CAP^N.

DISCUSSION

It is generally thought that changes in protein shape and bonding interactions, which are considered to primarily contribute to enthalpy, are necessary to propagate binding signals to remote sites. Nevertheless, the possibility of allosteric regulation through dynamic (entropic) mechanisms has long been recognized[8,10,38]. On the basis

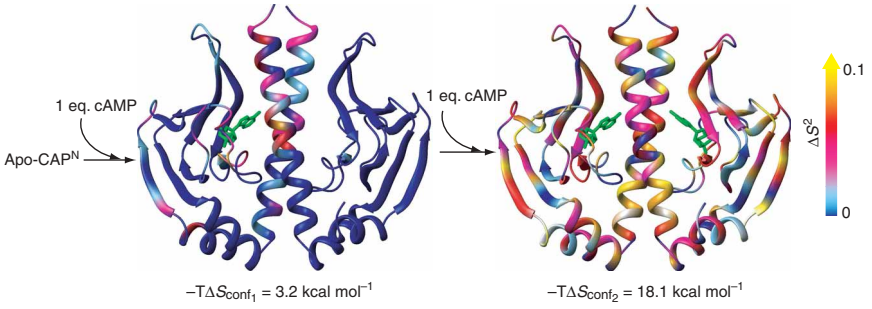

Figure 8 Effect of sequential binding of cAMP on order parameters of CAP^N. ΔS^2 is mapped by continuous-scale color onto structures; residues with negative ΔS^2 values are colored white. ΔS^2 is given as S^2 (after binding) – S^2 (before binding), so positive ΔS^2 values denote enhanced rigidity of the protein backbone upon binding. The conformational entropic penalty for binding of the second cAMP (18.1 kcal mol^{-1}) is much larger than the corresponding penalty for the first cAMP binding (3.2 kcal mol^{-1}). Values of ΔS^2 are plotted in **Supplementary Figure 6**.

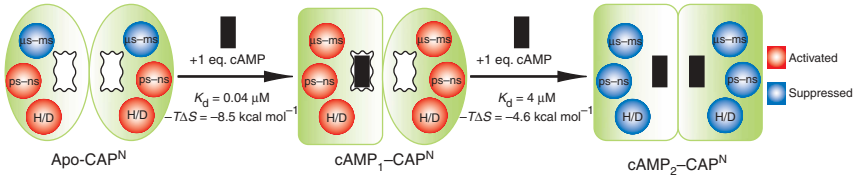

Figure 9 Overall effect of sequential cAMP binding on conformation and dynamics of CAP^N. In the absence of cAMP (apo state) CAP^N shows considerable flexibility on the ps–ns timescale and limited stability (enhanced H/D exchange rates). The cAMP-binding sites are also flexible (denoted by wavy lines). Binding of the first cAMP molecule has little effect on the ps–ns flexibility and H/D exchange rates, but it activates slow motions (μs–ms) of both subunits. Whereas the conformation of the liganded subunit of cAMP$_1$–CAP^N is extensively affected, that of the unliganded subunit is not perturbed. Subsequent binding of the second cAMP molecule greatly suppresses both slow and fast motions and increases stability (lower H/D exchange rates). The much lower favorable entropy change that accompanies the second cAMP binding compared with the first is the source of the negative cooperativity. Red and blue indicate activated and suppressed motions, respectively. Change in overall shape of each subunit represents a change in mean conformation.

of the present data (summarized in a model depicted in **Fig. 9**) we suggest that the cooperative binding of cAMP to CAP^N provides the first definitive example of a biological system wherein allosteric interactions are mediated exclusively by changes in protein motions.

Study of biological systems showing negative cooperativity allows, in principle, for isolation and characterization of intermediate states. Although few in number, crystallographic studies of such oligomeric systems have sometimes indicated that binding of the first ligand may distort the shape of the unliganded subunit, thereby rendering the binding of the second ligand more unfavorable[18,39]. Nevertheless, other crystallographic studies have not revealed any obvious structural effect on the unfilled subunit in the intermediate complex that could account for the observed negative cooperativity[18,40,41], raising the possibility that other mechanisms may act to increase the energy of the second binding step. Our NMR data show that, indeed, negative cooperativity can proceed with no conformational changes transmitted between the binding sites of the subunits.

Despite the fact that binding of cAMP to CAP^N does not induce long-range structural effects in the other subunit (**Fig. 2**), the motions of residues located at remote sites are clearly affected (**Figs. 3** and **5**). This observation is very important, because considering solely structural information provided by chemical shift perturbation, which is a very sensitive measure of changes in the average conformation, one would erroneously conclude that the core of the unliganded subunit does not 'sense' the presence of the ligand in the other subunit. It is particularly noteworthy that, although binding of the second cAMP molecule does not perturb the chemical shift of the other subunit, the motions of almost all residues throughout both subunits are extensively suppressed. Further, despite the fact that the unliganded subunit does not alter its mean conformation upon binding of the first cAMP to CAP^N (because $\Delta\delta \sim 0$), it shows enhanced flexibility involving excursions into alternate conformational states.

Notably, slow and fast motions of residues located at distant regions are affected in the absence of a visible connectivity pathway. This result further undermines the mechanical view of allosteric cooperativity, wherein binding effects are assumed to propagate through a series of conformational distortions. Rather, the ligand-induced redistribution of the protein's dynamic fluctuations affects regions linked by cooperative interactions (**Figs. 3** and **5**), thereby providing a means of propagating the allosteric signal to the distal site even in the absence of structural changes.

The thermodynamic basis of the observed anticooperative binding of cAMP to CAP^N is entirely of entropic nature (**Figs. 7** and **9**). Estimation of the conformational entropy from changes of order parameters (**Fig. 8**) indeed confirms that the calorimetrically measured difference in entropy between the two sequential binding steps is primarily due to alterations in protein flexibility. Despite the large unfavorable change in conformational entropy resulting from the suppression of protein motions, binding of the second cAMP is still entropy driven overall, as is the binding of the first cAMP molecule, most probably because of the large favorable solvation entropy change that accompanies the binding of hydrophobic ligands[9]. However, the larger conformational entropic penalty in the second step greatly decreases the total entropy of the system, resulting in weaker and, thus, anticooperative binding.

Earlier NMR studies have offered valuable insight into the potential role of dynamics in the function of two cooperative systems. Calcium binding to the singly calcium-liganded complex of the dimeric calbindin D_{9k} has been shown to result in suppression of fast motions in both subunits[15]. Despite the fact that considerable structural changes accompany binding of calcium to calbindin D_{9k} and that the thermodynamic basis of its cooperative binding remains unknown, these results highlight the potentially important role of protein motions. Another elegant study characterized anticooperative ligand binding to a dimeric enzyme[14]. Although the limited stability of the system did not permit the authors to measure fast motions and order parameters, they demonstrated that slow (μs–ms) timescale motions are quenched only upon binding of the second ligand[14]. Regrettably, there is currently no theory to relate these motions to the spatial amplitudes of the underlying conformational phenomena, and therefore no quantitative assessment of entropy can be made. As has been noted[8], μs–ms dynamics are typically considered to reflect cooperative transitions between two states, implying that the contribution of these dynamic modes to the change in entropy may be very small.

In sum, the cooperative binding of cAMP to CAP^N provides the first definitive example of a system wherein allosteric interactions are exclusively mediated by changes in protein motions. Therefore, the present findings provide direct support for the existence of biological systems that show purely dynamics-driven allostery. The large amount of residual entropy detected experimentally in proteins[8,9,42] suggests that such an allosteric mechanism may be more common than previously thought.

METHODS

Sample preparation. The His$_6$-tagged CAP^N domain (residues 1–138) was amplified by PCR, using as a template the pAKCRP plasmid that encodes wild-type *E. coli* CAP (residues 1–209), and transformed into BL21(DE3) cells. Isotopically labeled samples for NMR studies were prepared by growing the cells in M9 media in the presence of ampicillin. For the backbone assignment, a U-^{2}H,^{15}N,^{13}C-labeled sample was prepared by supplementing the growing media with 1 g l^{-1} of $^{15}NH_4Cl$ and 2 g l^{-1} $^2H_7$,$^{13}C_6$-glucose in 99.9% D_2O. For the relaxation experiments, a U-^{2}H,^{15}N-labeled sample was prepared using 1 g l^{-1} of $^{15}NH_4Cl$ and 2 g l^{-1} $^2H_7$,$^{12}C_6$-glucose in 99.9% D_2O. Two purification steps were used for all protein samples. The first involved a nickel-chelated sepharose fast-flow resin (Amersham) and the second a Superdex-200 size-exclusion column (Amersham). Protein concentration was determined

spectrophotometrically at 278 nm using an extinction coefficient of 36,900 M^{-1} cm^{-1}. cAMP concentration was determined spectrophotometrically at 259 nm using a molecular extinction coefficient of 14,650 M^{-1} cm^{-1}. Protein concentration for samples used for NMR studies was typically 0.4 mM. The singly ($cAMP_1$–CAP^N) and doubly ($cAMP_2$–CAP^N) liganded complexes were prepared by using cAMP/CAP^N molar ratios of 1:1 and 2:1, respectively. The strong binding of cAMP to CAP^N for both steps (K_{d1} = 0.04 μM and K_{d2} = 4 μM, for the first and second binding steps, respectively) and the strong negative cooperativity ensures that, at a cAMP/CAP^N ratio of 1:1, one subunit of CAP^N is completely saturated and the other completely empty. Similarly, at a cAMP/CAP^N ratio of 2:1, both subunits are saturated, in the absence of excess of cAMP.

NMR assignment. All NMR spectra were recorded at 30 °C on a Varian 600-MHz spectrometer. Sequential assignment of the ^1H, ^{13}C and ^{15}N protein chemical shifts in apo-CAP^N, $cAMP_1$–CAP^N and $cAMP_2$–CAP^N was achieved by means of through-bond heteronuclear scalar correlations along the backbone using a set of 3D HNCA, HN(CO)CA, HNCACB and HN(CO)CACB experiments. The combined chemical shift change of a particular residue upon ligand binding was calculated as:

$$\Delta\delta = \sqrt{(\omega_{HN}\Delta\delta_{HN})^2+(\omega_N\Delta\delta_N)^2+(\omega_{C\alpha}\Delta\delta_{C\alpha})^2+(\omega_{C\beta}\Delta\delta_{C\beta})^2+(\omega_{CO}\Delta\delta_{CO})^2} \quad (1)$$

where ω_i denotes the weight factor of nucleus i; $\omega_{HN} = 1$, $\omega_N = 0.154$, $\omega_{C\alpha} = \omega_{C\beta} = 0.276$ and $\omega_{CO} = 0.341$ (ref. 43).

Relaxation measurement and analysis. Four relaxation parameters were measured for all backbone amides of CAP^N in the apo, singly liganded and doubly liganded states: the ^1H-^{15}N NOE, the longitudinal relaxation time T_1, the transverse relaxation time T_2 and the rotating-frame longitudinal relaxation time $T_{1\rho}$. ^{15}N relaxation dispersion T_2-CPMG data were recorded for the $cAMP_1$–CAP^N complex. Data sets were acquired as 256 × 1,024 complex points in the $t_1 \times t_2$ time-domain dimensions. Data points were fitted as a function of the length of the parametric relaxation delay to two-parameter decay curves of the form $I(t) = I_0e^{-Rt}$, where I is the intensity of the magnetization. The error in the rate constant was assessed from Monte Carlo simulations. ^1H-^{15}N NOE data were obtained by recording, in an interleaved manner, one spectrum with a 5-s recycle delay followed by a 5-s saturation and another spectrum with no saturation and a 10-s recycle delay. Representative relaxation data were recorded at three different protein concentrations (0.05, 0.4 and 1.05 mM) to exclude contributions from protein aggregation. The final relaxation data were recorded using a 0.4 mM protein sample.

To characterize and quantify exchange contributions, R_{ex}, both the rotating-frame[44] and T_2-CPMG[27] relaxation-dispersion data were recorded. In both cases, R_{ex} is measured independently of the presence of anisotropy and any change that ligand binding may elicit in the overall tumbling of the protein. These NMR experiments measure the excess transverse relaxation rate, R_{ex}, caused by the exchange of nuclei between different conformations or states with different chemical shifts. The similarity of exchange rates extracted from fits of dispersion profiles on a per-residue basis (**Fig. 4**) supports a two-state model of exchange.

To probe fast motions that take place on the ps–ns timescale, we used the reduced spectral density mapping approach[45], which makes no assumptions a priori regarding the molecular anisotropy or internal motions. Briefly, the relation between the relaxation rates and the spectral density function, $J(\omega)$, is used to extract values of the latter, with the use of T_1, T_2 and the cross-relaxation rate, σ. At high frequencies (>400 MHz), $J(\omega)$ varies very little and the three spectra densities $J(\omega_H + \omega_N)$, $J(\omega_H)$ and $J(\omega_H - \omega_N)$ may be averaged to one average spectra density, $\langle J(\omega_H)\rangle$, in which ω_H and ω_N are the ^1H and ^{15}N Larmor frequencies, respectively. The frequency in $\langle J(\omega_H)\rangle$ may be taken equal to $0.87\omega_H$. The value of the spectral density function at $0.87\omega_H$ frequency is the most diagnostic for ps–ns motions.

Assessment of conformational entropy from order parameters. The contribution of protein motions to the conformational entropy ($-T\Delta S_{conf}$) of cAMP binding to CAP^N was estimated by measuring changes in the order parameter, S^2, as a function of the ligation state. Because of the complex dynamics observed in the CAP system, reduced-spectral density mapping was used to calculate S^2, as described[37,46]. This approach has been applied successfully before in calculating the conformational entropy contribution to the association entropy of a protein–DNA complex[37]. A local overall rotational correlation time, τ_M, is obtained from the spectral density function as:

$$\tau_M = \omega_N^{-1}((J(0) - J(\omega_N))/J(\omega_N))^{1/2} \quad (2)$$

Once a value of τ_M has been determined, the amplitude of intramolecular motion of the N-H bond vector in a molecular reference frame is given by:

$$S^2 = 5(J(0) - J(\omega_N))(1 + \omega_N^2\tau_M^2)/2\omega_N^2\tau_M^3 \quad (3)$$

As shown previously, the parameter S^2 of equation (3) is a very good approximation of the square of the generalized order parameter extracted by the model-free spectral density function[37,46,47]. In the case of ribonuclease H, for example, S^2 values calculated from equation (3) and using the full model-free formalism have a linear correlation coefficient of 0.97 (ref. 37). The conformational entropy of the CAP^N backbone is then calculated by[36]:

$$\Delta S = -k_B \sum_i \ln\left\{\frac{3 - (1 + 8S_{a,i})^{1/2}}{3 - (1 + 8S_{b,i})^{1/2}}\right\} \quad (4)$$

in which k_B is the Boltzmann constant and S_a and S_b are the order parameters for state a (for example, apo-CAP^N) and state b (for example, $cAMP_1$–CAP^N). Accurate extraction of order parameters is crucially dependent on identifying and separating the chemical-exchange contribution. In our study, this has been done by recording rotating frame and T_2-CPMG relaxation dispersion, so the T_2 values used for obtaining $J(0)$ have been corrected for the exchange term R_{ex}.

Determination of exchange rates. Amide proton exchange rates were determined from the time course of the peak intensities in a series of ^1H-^{15}N HSQC spectra after dissolving lyophilized samples in D_2O. The final pD was adjusted by DCl or NaOD solutions and was measured with a glass electrode at the temperature of the exchange experiment, taking into account the isotope effect: $pD = pH_{read} + 0.4$. Exchange rates were determined by plotting the intensities of each residue against time and fit to a first-order rate expression.

ITC experiments. Calorimetric titrations of CAP^N with cAMP were performed on a VP-ITC microcalorimeter (MicroCal). Protein samples were extensively dialyzed against ITC buffer containing 50 mM potassium phosphate (pH 6.0), 500 mM KCl and 1 mM Tris(2-carboxyethyl)phosphine (TCEP). All solutions were filtered using membrane filters (pore size 0.45 μm) and thoroughly degassed for 20 min by gentle stirring under vacuum. The 1.35-ml sample cell was filled with a 30 μM solution of protein and the 250-μl injection syringe with 0.6 mM of the titrating cAMP. The ligand solution was prepared by dissolving cAMP in the flow-through of the last buffer exchange. Each titration typically consisted of a preliminary 2-μl injection followed by 30 subsequent 8-μl injections. Data for the preliminary injection, which are affected by diffusion of the solution from and into the injection syringe during the initial equilibration period, were discarded. Binding isotherms were generated by plotting heats of reaction normalized by the modes of injectant versus the ratio of total injectant to total protein per injection. The data were fit using the sequential binding site model embedded in Origin 7.0 (Microcal).

Note: Supplementary information is available on the Nature Structural & Molecular Biology website.

ACKNOWLEDGMENTS

We thank P. Loria (Yale) and P. Huskey (Rutgers) for providing us with scripts for the analysis of some of the relaxation data. This work was supported by US National Science Foundation grant MCB-0618259 to C.G.K. and by US National Institutes of Health grant GM41376 and a Howard Hughes Medical Institute investigatorship to R.H.E.

COMPETING INTERESTS STATEMENT

The authors declare that they have no competing financial interests.

Published online at http://www.nature.com/nsmb/
Reprints and permissions information is available online at http://npg.nature.com/reprintsandpermissions/

1. Hardy, J.A. & Wells, J.A. Searching for new allosteric sites in enzymes. *Curr. Opin. Struct. Biol.* **14**, 706–715 (2004).
2. Gao, Z.G. & Jacobson, K.A. Allosterism in membrane receptors. *Drug Discov. Today* **11**, 191–202 (2006).
3. Swain, J.F. & Gierasch, L.M. The changing landscape of protein allostery. *Curr. Opin. Struct. Biol.* **16**, 102–108 (2006).
4. Suel, G.M., Lockless, S.W., Wall, M.A. & Ranganathan, R. Evolutionarily conserved networks of residues mediate allosteric communication in proteins. *Nat. Struct. Biol.* **10**, 59–69 (2003).
5. Koshland, D.E., Jr. Conformational changes: how small is big enough? *Nat. Med.* **4**, 1112–1114 (1998).
6. Changeux, J.P. & Edelstein, S.J. Allosteric mechanisms of signal transduction. *Science* **308**, 1424–1428 (2005).
7. Bray, D. & Duke, T. Conformational spread: the propagation of allosteric states in large multiprotein complexes. *Annu. Rev. Biophys. Biomol. Struct.* **33**, 53–73 (2004).
8. Wand, A.J. Dynamic activation of protein function: a view emerging from NMR spectroscopy. *Nat. Struct. Biol.* **8**, 926–931 (2001).
9. Homans, S.W. Probing the binding entropy of ligand-protein interactions by NMR. *ChemBioChem* **6**, 1585–1591 (2005).
10. Cooper, A. & Dryden, D.T. Allostery without conformational change. A plausible model. *Eur. Biophys. J.* **11**, 103–109 (1984).
11. Freire, E. The propagation of binding interactions to remote sites in proteins: analysis of the binding of the monoclonal antibody D1.3 to lysozyme. *Proc. Natl. Acad. Sci. USA* **96**, 10118–10122 (1999).
12. Pan, H., Lee, J.C. & Hilser, V.J. Binding sites in *Escherichia coli* dihydrofolate reductase communicate by modulating the conformational ensemble. *Proc. Natl. Acad. Sci. USA* **97**, 12020–12025 (2000).
13. Kern, D. & Zuiderweg, E.R. The role of dynamics in allosteric regulation. *Curr. Opin. Struct. Biol.* **13**, 748–757 (2003).
14. Stevens, S.Y., Sanker, S., Kent, C. & Zuiderweg, E.R. Delineation of the allosteric mechanism of a cytidylyltransferase exhibiting negative cooperativity. *Nat. Struct. Biol.* **8**, 947–952 (2001).
15. Maler, L., Blankenship, J., Rance, M. & Chazin, W.J. Site-site communication in the EF-hand Ca2+-binding protein calbindin D9k. *Nat. Struct. Biol.* **7**, 245–250 (2000).
16. Lee, A.L., Kinnear, S.A. & Wand, A.J. Redistribution and loss of side chain entropy upon formation of a calmodulin-peptide complex. *Nat. Struct. Biol.* **7**, 72–77 (2000).
17. Fuentes, E.J., Der, C.J. & Lee, A.L. Ligand-dependent dynamics and intramolecular signaling in a PDZ domain. *J. Mol. Biol.* **335**, 1105–1115 (2004).
18. Koshland, D.E., Jr. The structural basis of negative cooperativity: receptors and enzymes. *Curr. Opin. Struct. Biol.* **6**, 757–761 (1996).
19. Brown, A.M. & Crothers, D.M. Modulation of the stability of a gene-regulatory protein dimer by DNA and cAMP. *Proc. Natl. Acad. Sci. USA* **86**, 7387–7391 (1989).
20. Harman, J.G. Allosteric regulation of the cAMP receptor protein. *Biochim. Biophys. Acta* **1547**, 1–17 (2001).
21. Passner, J.M., Schultz, S.C. & Steitz, T.A. Modeling the cAMP-induced allosteric transition using the crystal structure of CAP-cAMP at 2.1 A resolution. *J. Mol. Biol.* **304**, 847–859 (2000).
22. Heyduk, E., Heyduk, T. & Lee, J.C. Intersubunit communications in *Escherichia coli* cyclic AMP receptor protein: studies of the ligand binding domain. *Biochemistry* **31**, 3682–3688 (1992).
23. Akke, M. NMR methods for characterizing microsecond to millisecond dynamics in recognition and catalysis. *Curr. Opin. Struct. Biol.* **12**, 642–647 (2002).
24. Volkman, B.F., Lipson, D., Wemmer, D.E. & Kern, D. Two-state allosteric behavior in a single-domain signaling protein. *Science* **291**, 2429–2433 (2001).
25. Kalodimos, C.G. *et al.* Structure and flexibility adaptation in nonspecific and specific protein-DNA complexes. *Science* **305**, 386–389 (2004).
26. Keramisanou, D. *et al.* Disorder-order folding transitions underlie catalysis in the helicase motor of SecA. *Nat. Struct. Mol. Biol.* **13**, 594–602 (2006).
27. Mulder, F.A., Mittermaier, A., Hon, B., Dahlquist, F.W. & Kay, L.E. Studying excited states of proteins by NMR spectroscopy. *Nat. Struct. Biol.* **8**, 932–935 (2001).
28. Forman-Kay, J.D. The 'dynamics' in the thermodynamics of binding. *Nat. Struct. Biol.* **6**, 1086–1087 (1999).
29. Cavanagh, J. & Akke, M. May the driving force be with you–whatever it is. *Nat. Struct. Biol.* **7**, 11–13 (2000).
30. Zidek, L., Novotny, M.V. & Stone, M.J. Increased protein backbone conformational entropy upon hydrophobic ligand binding. *Nat. Struct. Biol.* **6**, 1118–1121 (1999).
31. Stone, M.J. NMR relaxation studies of the role of conformational entropy in protein stability and ligand binding. *Acc. Chem. Res.* **34**, 379–388 (2001).
32. Igumenova, T.I., Frederick, K.K. & Wand, A.J. Characterization of the fast dynamics of protein amino acid side chains using NMR relaxation in solution. *Chem. Rev.* **106**, 1672–1699 (2006).
33. Hilser, V.J., Garcia-Moreno, E.B., Oas, T.G., Kapp, G. & Whitten, S.T. A statistical thermodynamic model of the protein ensemble. *Chem. Rev.* **106**, 1545–1558 (2006).
34. Gekko, K., Obu, N., Li, J. & Lee, J.C. A linear correlation between the energetics of allosteric communication and protein flexibility in the *Escherichia coli* cyclic AMP receptor protein revealed by mutation-induced changes in compressibility and amide hydrogen-deuterium exchange. *Biochemistry* **43**, 3844–3852 (2004).
35. Englander, J.J., Louie, G., McKinnie, R.E. & Englander, S.W. Energetic components of the allosteric machinery in hemoglobin measured by hydrogen exchange. *J. Mol. Biol.* **284**, 1695–1706 (1998).
36. Yang, D. & Kay, L.E. Contributions to conformational entropy arising from bond vector fluctuations measured from NMR-derived order parameters: application to protein folding. *J. Mol. Biol.* **263**, 369–382 (1996).
37. Bracken, C., Carr, P.A., Cavanagh, J. & Palmer, A.G., III Temperature dependence of intramolecular dynamics of the basic leucine zipper of GCN4: implications for the entropy of association with DNA. *J. Mol. Biol.* **285**, 2133–2146 (1999).
38. Gunasekaran, K., Ma, B. & Nussinov, R. Is allostery an intrinsic property of all dynamic proteins? *Proteins* **57**, 433–443 (2004).
39. Anderson, A.C., O'Neil, R.H., DeLano, W.L. & Stroud, R.M. The structural mechanism for half-the-sites reactivity in an enzyme, thymidylate synthase, involves a relay of changes between subunits. *Biochemistry* **38**, 13829–13836 (1999).
40. Leslie, A.G. & Wonacott, A.J. Structural evidence for ligand-induced sequential conformational changes in glyceraldehyde 3-phosphate dehydrogenase. *J. Mol. Biol.* **178**, 743–772 (1984).
41. Hampele, I.C. *et al.* Structure and function of the dihydropteroate synthase from *Staphylococcus aureus*. *J. Mol. Biol.* **268**, 21–30 (1997).
42. Lee, A.L. & Wand, A.J. Microscopic origins of entropy, heat capacity and the glass transition in proteins. *Nature* **411**, 501–504 (2001).
43. Evenas, J. *et al.* Ligand-induced structural changes to maltodextrin-binding protein as studied by solution NMR spectroscopy. *J. Mol. Biol.* **309**, 961–974 (2001).
44. Korzhnev, D.M., Skrynnikov, N.R., Millet, O., Torchia, D.A. & Kay, L.E. An NMR experiment for the accurate measurement of heteronuclear spin-lock relaxation rates. *J. Am. Chem. Soc.* **124**, 10743–10753 (2002).
45. Farrow, N.A., Zhang, O., Szabo, A., Torchia, D.A. & Kay, L.E. Spectral density function mapping using ^{15}N relaxation data exclusively. *J. Biomol. NMR* **6**, 153–162 (1995).
46. Lefevre, J.F., Dayie, K.T., Peng, J.W. & Wagner, G. Internal mobility in the partially folded DNA binding and dimerization domains of GAL4: NMR analysis of the N-H spectral density functions. *Biochemistry* **35**, 2674–2686 (1996).
47. Krizova, H., Zidek, L., Stone, M.J., Novotny, M.V. & Sklenar, V. Temperature-dependent spectral density analysis applied to monitoring backbone dynamics of major urinary protein-I complexed with the pheromone 2-sec-butyl-4,5-dihydrothiazole. *J. Biomol. NMR* **28**, 369–384 (2004).